Indonesian Journal of Electrical Engineering and Informatics (IJEEI)
Vol. 11, No. 1, March 2023, pp. 133~151
ISSN: 2089-3272, DOI: 10.52549/ijeei.v11i1.3931

Multimachine Stability Enhancement Using Fuzzy- Logic Based PSS Tuning With Shunt FACTS Device

M Madhusudhan [1], H Pradeepa [2], M V Likith Kumar [3], Srishail K Bilgundi[4]
[1, 2, 3, 4] Department of Electrical and Electronics Engineering, The National of Engineering, Mysore, Karnataka, India-570008

Article Info

Article history:

Received Jun 16, 2022
Revised Feb 12, 2023
Accepted Feb 23, 2023

Keyword:

Power system stabilizer (PSS)
Flexible Alternating Current Transmission system(FACTS)
Voltage Source Converter (VSC)
Static-Synchronous Compensator(STATCOM)

ABSTRACT

In Large power system network the dynamic behaviour of system is nonlinear in nature. Due to disturbance the system stability cannot be maintained, which leads to outage of power equipment. In order to restore the system parameter after perturbance, coordination control damping is essential. Coordination control damping can be achieved by using fuzzy based PSS and STATCOM in multimachine system for sever disturbance. Due to perturbance the system loss its synchronism and the system parameter deviate from the nominal value. With the effective damping control technique proposed in this article is to minimize the integral square error of speed deviation. Two area 4-Machine 11-bus test system considered and the simulation of proposed system is developed in Matlab/Simulink R2018a.

Corresponding Author:

Dr. H Pradeepa
Department of Electrical and Electronics Engineering,
The National of Engineering, Mysore,Karnataka,India-570008
Email: pradeep3080@nie.ac.in

1. INTRODUCTION

Power system stability refers to a system's ability to return to its operating state after a disturbance. The stability of the power system is crucial since the generator might not be able to handle the connected load due to perturbation [1]. Power systems are operated at or close to maximum capacity to fulfil the expanding demands for electricity, which are rising quickly. Sustaining such power grids' reliable operation in the face of various small- and large-scale power network disturbances is of utmost importance [2]. After the disturbance has subsided, the oscillations in the power system are not completely dampened out, and the system is unable to return to its equilibrium point. This poses a serious threat to the network's power systems, including the heating or malfunction of equipment and a shortening of its operational life. Consequently, transients, machine speed deviations, and load angle deviations are the end effects of the power system's instability, and they lead to inappropriate power transfer in the given network [3-4].

An efficient controller design for multi-machine power systems is required to regulate nonlinear oscillation in the operating network. Power system stabiliser (PSS), which is often installed in the excitation system with the generator, serves as the main damping control in the power system. [5]. Nevertheless, PSS alone cannot offer the necessary damping for a variety of power system events. Consequently, for a multi-machine power system to function properly, an advanced controller and coordination approach must be developed in addition to PSS. Using FACTS will help you achieve this [6-7]. The stability of multi-machine control systems is impacted by the presence of inter-area oscillation modes. FACTS-based damping techniques are increasingly used in these modes [8].

Local and inter-area oscillation patterns are frequently seen in multimachine systems. These oscillations cause variations in the generator terminal voltage, power level, frequency, rotor angle deviation, and all other variables [9]. Very few cycle oscillations have a larger frequency range of 0.7-3.0 Hz and are local area mode oscillations. On the other hand, large cycle oscillations are inter-area mode oscillations with low frequency between 0.1 and 0.7 Hz [10]. Today, an appropriate control optimization technique created specifically for PSS is used to dampen down power system oscillations [11-15]. A crucial aspect of controlling the dynamics of the power system is PSS coordination with the FACTS device. [16-17]. For large power systems, a single VSC-based STATCOM is a good alternative to improve voltage profile and obtain additional damping to reduce rotor oscillation. [18-20].

The versatility and speed of VSC-based STATCOM have prompted a significant amount of research interest. A VSC with a connected DC supply through a capacitor makes up the regulated reactive power source known as STATCOM. When used in capacitive mode, STATCOM can generate reactive power; when used in inductive mode, it can absorb reactive power. STATCOM is a shunt device connected to the grid by a coupling transformer. [21-23]. A more interesting part of STATCOM is its ability to inject steady current even when the system's terminal voltage is less than 0.5 p.u [24]. The primary benefit of STATCOM is that it offers quick grid voltage collapse management, and STATCOM can deliver continuous reactive power regardless of grid voltage [25-27]. The impact of power electronics converters in the power system restricts the peak of rotor swing in STATCOM, which is essentially a VSC-based power electronic device [28]. An IEEE 11 bus system was used as the testing system in this investigation. To minimise the performance index with respect to generator speed deviation, fuzzy rule matrix-based PSS has been created. Integral square error is decreased to increase the stability of multimachine systems [29-30]. The linearization and state space analysis of the multimachine machine system and FACTS devices is given with mathematical modelling [31].

1.1. Generator Excitation System Equipped with PSS

An excitation system is a device that delivers field current to the rotor winding of a generator. Figure 1 shows the fundamental construction of a generator excitation system. Well-designed excitation systems provide dependable and consistent operation, stability, and quick transient response. An automated voltage regulator (AVR) is a thyristor-based controlled rectifier that regulates the voltage at the generator output terminals while also exciting the generator. The governor of a steam turbine is a part of the turbine control system that controls rotational speed in response to changing load circumstances.

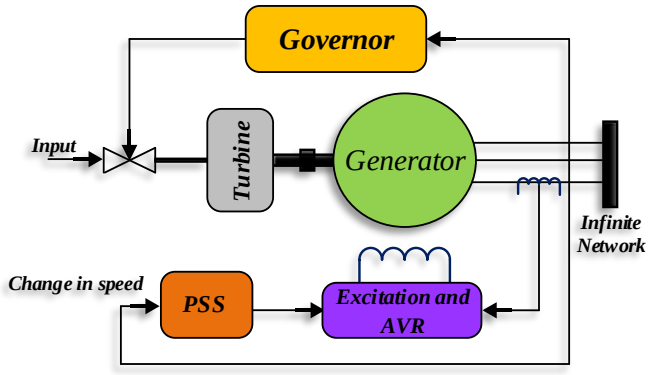

Figure 1. Basic Structure of Generator Excitation with PSS

2. MODELLING OF GENERATOR AND STATCOM

2.1. Modelling of Generator in Differential algebraic equation

The excitation system can be expressed as:

$$T_{Ei}\frac{dE_{fdi}}{dt} = -(K_{Ei} + S_{Ei}(E_{fdi}))E_{fdi} + V_{Ri} \quad (1)$$

$$T_{Fi}\frac{dR_{fi}}{dt} = -R_{fi} + \frac{K_{fi}}{T_{fi}}E_{fdi} \quad (2)$$

$$T_{Ai}\frac{dV_{Ri}}{dt} = -V_{Ri} + K_{Ai}R_{fi} - \frac{K_{Ai}K_{fi}}{T_{fi}}E_{fdi} + K_{Ai}(V_{refi} - V_i) \quad (3)$$

Generator Dynamics [31]

$$T'_{doi}\frac{dE'_{qi}}{dt} = E_{fdi} - (X_{di} - X'_{di})\{i_{di} - \frac{(X'_{di} - X''_{di})}{(X'_{di} - X_{ls})^2}\left(\Psi_{1di} + (X'_{di} - X_{ls})i_{di} - E'_{qi}\right\} \quad (4)$$

$$T''_{doi}\frac{d\Psi_{1di}}{dt} = -\Psi_{1di} + E'_{qi} - (X'_{di} - X_{ls})i_{di} \quad (5)$$

$$T'_{qoi}\frac{dE'_{di}}{dt} = -E'_{di} + \left(X_{qi} - X'_{qi}\right)\{i_{qi} - \frac{(X'_{qi} - X''_{qi})}{(X'_{qi} - X_{ls})^2}\left(\Psi_{2di} + (X'_{qi} - X_{ls}\right) i_{qi} - E'_{di}\} \quad (6)$$

$$T''_{qoi}\frac{d\Psi_{2di}}{dt} = -\Psi_{2di} - E'_{di} - \left(X'_{qi} - X_{ls}\right)i_{qi} \quad (7)$$

$$\frac{d\delta_i}{dt} = \omega_i - \omega_s \quad (8)$$

$$\frac{2H_i}{\omega_s}\frac{d\omega_i}{dt} = T_{Mi} - \frac{(X''_{di} - X_{ls})}{(X'_{di} - X_{ls})}E'_{qi}i_{qi} - \frac{(X'_{di} - X''_{di})}{(X'_{di} - X_{ls})}\Psi_{1di}i_{qi} - \frac{(X''_{qi} - X_{ls})}{(X'_{qi} - X_{ls})}E'_{di}i_{di} + \frac{(X'_{qi} - X''_{qi})}{(X'_{qi} - X_{ls})}\Psi_{2qi}i_{di} - (X''_{qi} - X''_{di})\, i_{di}i_{qi} - T_{FW} \quad (9)$$

The d-q frame terminal voltage and armature can be used to express the generator's electric output power:

$$P_e = V_{td}I_d + V_{tq}I_q \quad (10)$$

2.2. STATCOM state equation

$$\dot{V_{dc}} = \frac{I_{dc}}{C} = \frac{g(I_{sd}\cos\phi + I_{sq}\sin\phi)}{C} \quad (11)$$

Output of Voltage Source Converter is variable AC voltage with a controllable phase angle, which is expressed as

$$V_o = gV_{dc}\angle\phi \quad (12)$$

Where $g = m_i k$, while m_i is modulation index which depends on the pulse width of the PWM signal. k is ratio of AC to DC voltage.

Magnitude and phase of an AC output voltage of VSC can be controlled by the magnitude of DC voltage link and modulation index. Real power exchange between grid and STATCOM is done by controlling the VSC phase angle. Similarly, the reactive power can be supplied to the grid when magnitude of STATCOM voltage is more than Grid voltage.

The d-axis and q-axis component of STATCOM current can expressed as:

$$I_{ds} = \frac{a_1 E'_q - a_1 C V_{dc}\sin\phi - V_b\cos\phi}{a_1 X'_d + a_3} \quad (13)$$

$$I_{qs} = \frac{a_2 C V_{dc}\cos\phi + V_b\sin\phi}{a_1 X_d + a_3} \quad (14)$$

Where a_1, a_2 and a_3 are constants

The linearized model of proposed power system is given as follows:

$$\Delta\dot{\delta} = \omega_s\Delta\omega \quad (15)$$

$$\Delta\dot{\omega} = \frac{\Delta P_m - \Delta P_e}{M} \quad (16)$$

$$\Delta\dot{E'}_q = \frac{\Delta E_{fd} - (X_d - X_d')\Delta i_d - \Delta E'_q}{T'_{do}} \quad (17)$$

$$\Delta P_e = k_{p\delta}\Delta\delta + k_{peq}\Delta E'_q + k_{pdc}\Delta V_{dc} + k_{pg}\Delta g + k_{p\phi}\Delta\phi \quad (18)$$

$$\Delta V_t = k_{v\delta}\Delta\delta + k_{veq}\Delta E'_q + k_{vdc}\Delta V_{dc} + k_{vg}\Delta g + k_{v\phi}\Delta\phi \quad (19)$$

$$\Delta \dot{V_{dc}} = h_\delta \Delta\delta + h_{eq}\Delta E'_q + h_{dc}\Delta V_{dc} + h_g \Delta g + h_\phi \Delta\phi \quad (20)$$

$$\Delta V_{ac} = f_\delta \Delta\delta + f_{eq}\Delta E'_q + f_{dc}\Delta V_{dc} + f_g \Delta g + f_\phi \Delta\phi \quad (21)$$

Where $k, h,$ and f are constants of linearization
The power system linearization model with STATCOM in general is given by

$$\dot{X} = AX + BU \quad (22)$$

Where the state vector X is $[\Delta\delta, \Delta\omega, \Delta E'_q, \Delta E_{fd}, \Delta V_{dc}]^T$ and the control vector U is $[\Delta g, \Delta\phi]^T$.

3. INTEGRAL SQUARE ERROR OF GENERATOR

Integral square error is a measure of system performance that is calculated by integrating the square of error over a set time interval. In our case ISE is determined for the machine speed deviation, which is expressed for each generator given by

$$J_i = \int_0^\infty |\Delta\omega_i|^2 \quad (23)$$

Where subscript *i* indicated no. of generator in multimachine power system, *i* take value from 1 to 4. $\Delta\omega_i$ is corresponding machine speed deviation.

4. POWER SYSTEM STABILIZER

PSS is used to damp out the electromechanical mode of oscillation. To provide required damping for electro-mechanical oscillation we provide power system stabilizer. Block diagram of power system stabilizer is shown in figure 2

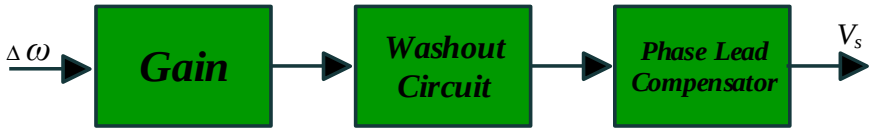

Figure 2. Structure of PSS

The speed deviation is derived from the generator parameter measurement block which is given as input to the PSS thus the name '$\Delta\omega$' PSS. PSS mainly consists of gain block, washout circuit, and the phase compensator. The phase lag between the exciter input and the air gap torque is compensated via PSS. The PSS is designed to correct for phase lag in order to achieve torque in phase with the speed variation.

4.1. Washout Circuit

The wash out circuit allows the high frequency signal to pass while blocking the steady state deviation. Figure 3 shows the block diagram of a washout circuit, commonly known as a high pass filter. T_w is the washout circuit's time constant.

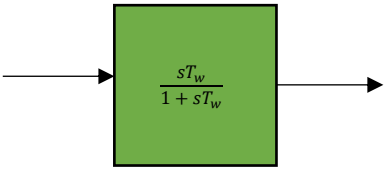

Figure 3. Washout Block

4.2. Lead-Lag Compensator

Figure 4 shows the basic function of this compensator is to provide the phase lead i.e., $T_1 > T_2$ and $T_3 > T_4$ where T_1, T_2, T_3 and T_4 are time constant of Phase compensator. If $T_2 > T_1$ and $T_4 > T_3$ the lag correction is then obtained. An operational amplifier is used to physically achieve phase correction. Local (0.7- 3.0Hz) and interarea (0.1-0.7Hz) oscillations must be dampened using a phase lead compensator that is properly designed. As a result, the frequency range of 0.1 to 3 Hz is damped out.

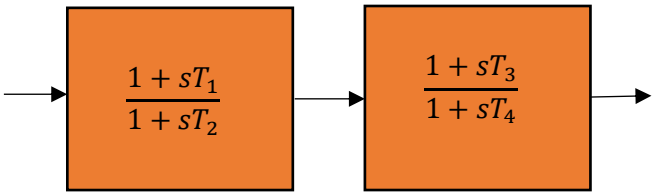

Figure 4. Lead-Lag Compensator

5. OBJECTIVES

- Dampen rotor oscillation.
- Maintaining generator terminal voltage within permissible limits.
- Maintaining machine synchronization.
- Minimize integral square error i.e., min J_i

6. METHODOLOGY

The mamdani basis fuzzy inference control is the most widely used fuzzy inference control, and it was the first control system based on fuzzy set theory. Mamdani fuzzy inferences are easy to understand, popular, and well-suited to human input. Fuzzification, interference, and defuzzification are the three primary process phases performed by the fuzzy controller. The membership function investigated here is speed deviation and change in speed deviation for desired control action initiated by PSS, and variables in the Fuzzification system are converted into linguistic rules. This linguistic variable, which is seven in this suggested study, has an inference method.

6.1. Fuzzy Logic Control Strategy for PSS

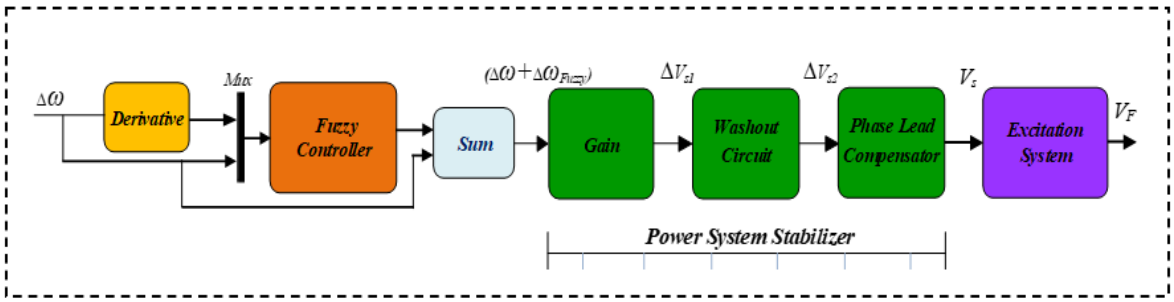

Figure 5. Fuzzy Logic Control based PSS

Linguistic variable and its limit ranges are assigned using the fuzzy rules indicated in Table 1. Linguistics rules has been transformed into output variable i.e., fuzzy control output the corresponding step is called defuzzification. Negative Medium (NM), Negative Big (NB), Negative Small (NS), Zero (ZR), Positive Small (PS), Positive Medium (PM) and Positive Big (PB) are the seven linguistic variables. The proposed control strategy as shown in Figure 5, while the membership functions are shown in Figures 6-9.

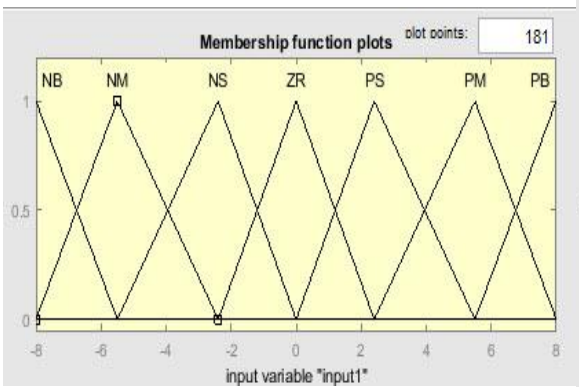

Figure 6. Control input1 membership function

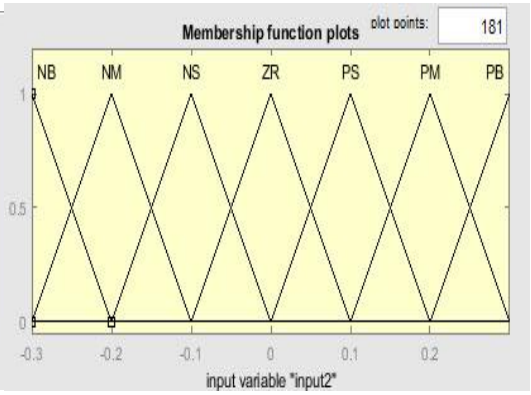

Figure 7. Control input2 membership function

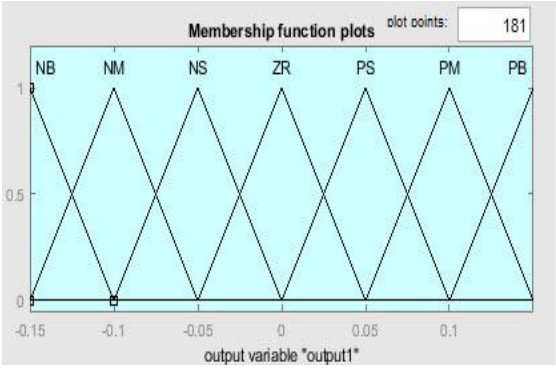

Figure 8. Control output membership function

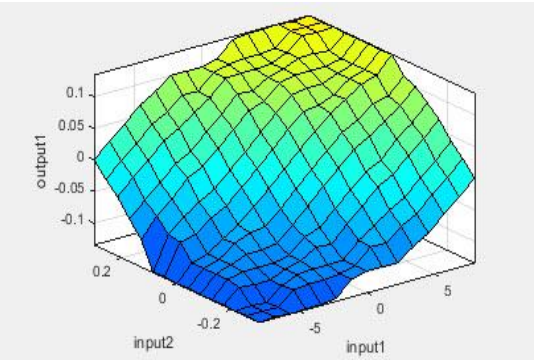

Figure 9. Surf view control and its inputs

Table 1. Fuzzy rule for two input membership function and control output

Speed Deviation	Change in Speed Deviation						
	NB	*NM*	*NS*	*ZR*	*PS*	*PM*	*PB*
NB	*NB*	*NB*	*NB*	*NB*	*NB*	*NS*	*ZR*
NM	*NB*	*NB*	*NM*	*NM*	*NS*	*ZR*	*PS*
NS	*NB*	*NM*	*NM*	*NS*	*ZR*	*PS*	*PM*
ZR	*NM*	*NM*	*NS*	*ZR*	*PS*	*PM*	*PM*
PS	*NM*	*NS*	*ZR*	*PS*	*PM*	*PM*	*PB*
PM	*ZS*	*ZR*	*PS*	*PM*	*PM*	*PB*	*PB*
PB	*ZR*	*PS*	*PM*	*PB*	*PB*	*PB*	*PB*

7. BENCHMARK

Figure 10 shows the benchmark system [21], which is made up of four generators: Gen1, Gen2, Gen3, and Gen 4, all of which are connected to bus 1, bus 2, bus 3, and bus 4, respectively. Each generator has a voltage level of 20kV and an MVA rating of 900MVA. Power transformers Trfx1, Trfx2, Trfx3, and Trfx4 each have an MVA rating of 900MVA and step up the generated voltage to 230kV at bus 5, bus 6, bus 10, and bus 11. A 10km nominal-pi transmission line is connected between buses (5 to 6) and buses (10 to 11). Similarly, a 25km nominal-pi transmission line connects buses (6 to 7) and buses (9 to 10), whereas a 220km nominal-pi transmission line and double circuit long transmission line connects bus (7 to 9). Where the one of long transmission line is split into two sections of 110km at middle of transmission line 3-ϕ circuit breaker is connected at bus 8. Constant impedance load of real power of 967MW, inductive reactive power of 100 Mvar & capacitive reactive power of -187Mvar at bus 7. Similarly real power of 1767MW inductive reactive power of 100 Mvar & capacitive reactive power of -187Mvar is connected bus 9.

7.1. Case Study

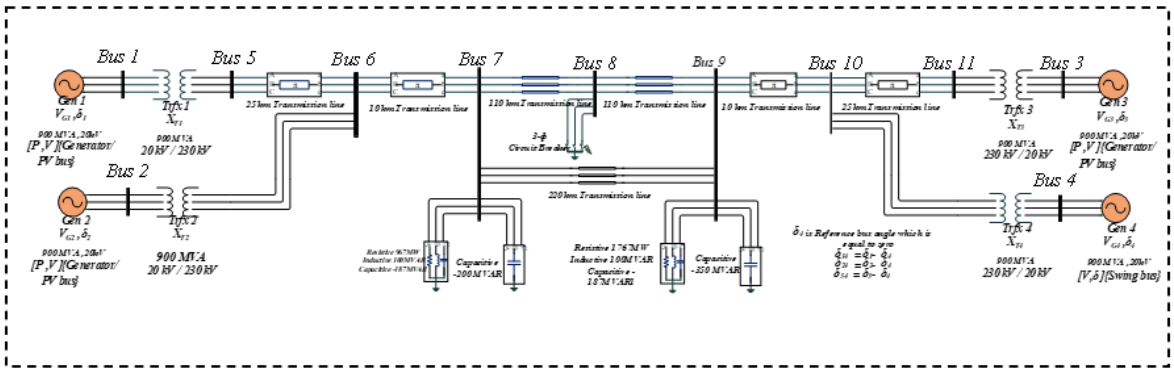

Figure 10. 4-Machine 11-Bus Test System

Table 2. The scenario of each case study

Fault Applied	Case study	PSS	Fuzzy Controller	STATCOM
LLL-G (12 cycles)	1	Absent	Absent	Absent
	2	Present	Absent	Absent
	3	Present	Present	Absent
	4	Present	Present	Present

The power oscillations of system parameters investigated in these case studies include rotor speed (Δω), rotor angle deviation ((Δδ), terminal voltage (Vg), and rotor speed (ω). In all of these circumstances, the 3-to-ground fault was triggered at 0.5 sec and cleared at 0.5+12/60, or 0.7 sec. So, the fault duration is 0.7-0.5 = 0.2 sec. Here power frequency is of 60Hz (T=16.6667 msec), where 16.66msec is require to complete 1 cycle. Thus for 0.2sec of 3-ϕ to ground fault 12 cycles are completed. The use of PSS, Fuzzy controller and STATCOM during fault for each study is explained in Table 2.

7.1.1. Case 1

The load angles of Machine 1, Machine 2, and Machine 3 are initially 36.34150799°, 24.95113671°, and 11.41908353°, respectively. However, as soon as a defect is initiated at bus 8, the load angle of the system starts to oscillate, as illustrated in Figure 11-13. It has been noted that the system becomes unstable when it is unable to return to its equilibrium point.

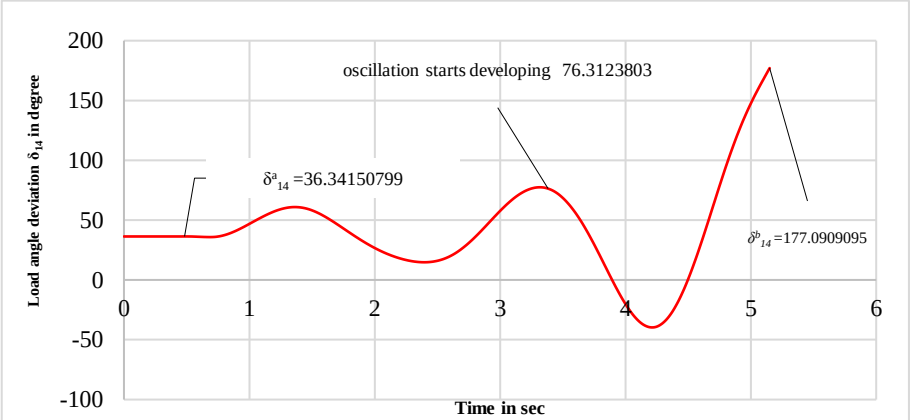

Figure 11. Power angle (δ_{14}) without PSS

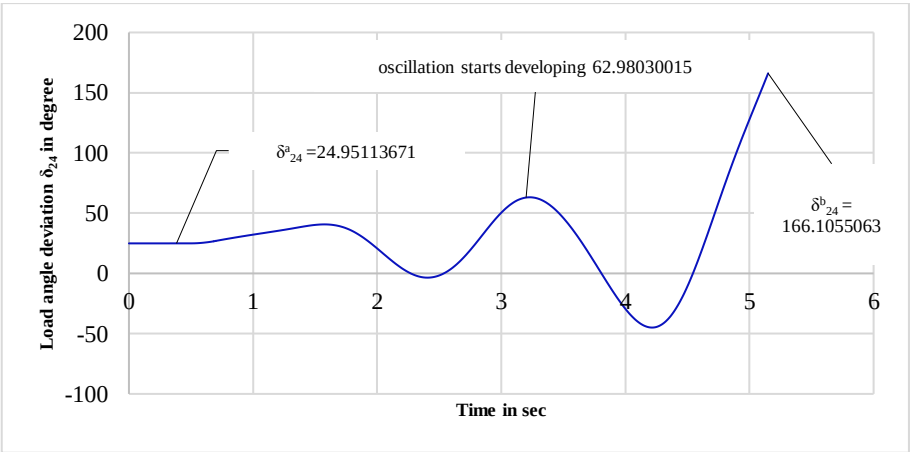

Figure 12. Power angle (δ_{24}) without PSS

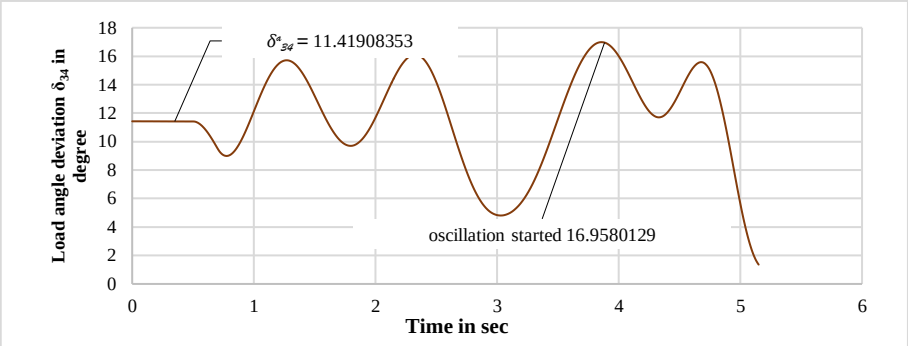

Figure 13. Power angle (δ_{34}) without PSS

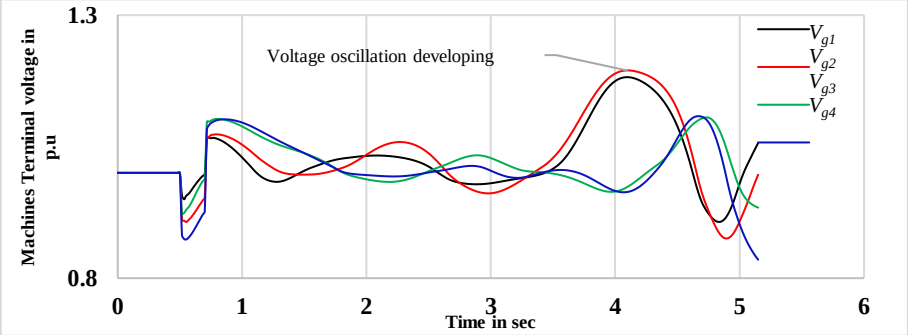

Figure 14. Terminal voltages of Machines without PSS

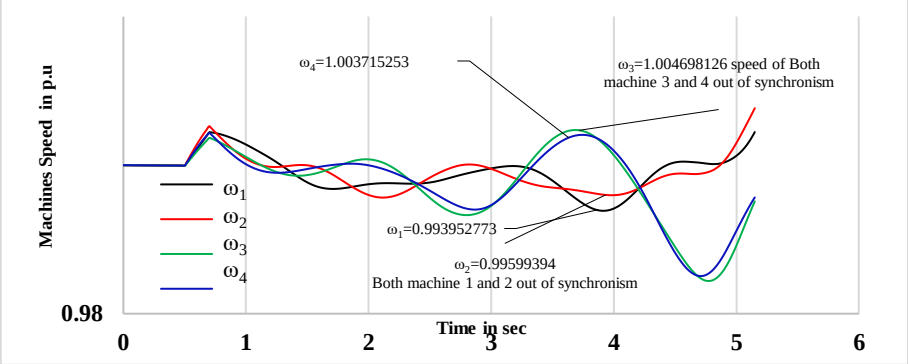

Figure 15. Machines Speed without PSS

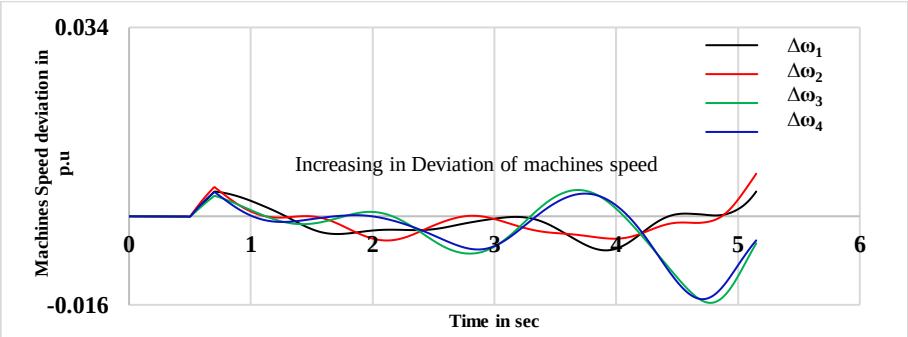

Figure 16. Machines Speed Deviation without PSS

Figure 14 shows how the terminal voltage of generators drops below the lowest allowable limit as soon as the fault is initiated. Yet, whenever the voltage oscillates, the system's security constraints are broken. So, even if the system voltage stability is not kept after the fault has been fixed, the generator's terminal voltage will overdamp as a result. Figure 15 provides a brief overview of each machine's speed in the power system. For the generator, the power system network is operated in synchronism in order to

provide frequency stabilisation. The synchronous machines' speeds start to deviate from one another when the system is disturbed. All of the speed profiles of each machine overlap, as we can see before problems, indicating. Machines 1 and 2 in region 1 and machines 3 and 4 in area 2 start to lose synchronism as soon as the fault is started, though. The speed deviation of all machines is seen in figure 16, where it starts to rise even after the issue has been fixed. Physically speaking, this means that the generator is accelerating and deaccelerating because each machine's speed is not returning to its initial speed. In this situation, the acceleration power of the machines starts to increase because it is not equal to zero.

7.1.2. Case 2

In this case the PSS is connected in the excitation system of generator which is used to damp out power system oscillation once the fault has been cleared. The load angle of machines is shown in Figures 17-19. The load angle of machines oscillates during fault and settle once the fault is cleared. However, it is observed that the settling time is large. The terminal voltages of machines without PSS as well as the respond with PSS is shown in Figures 20-22.

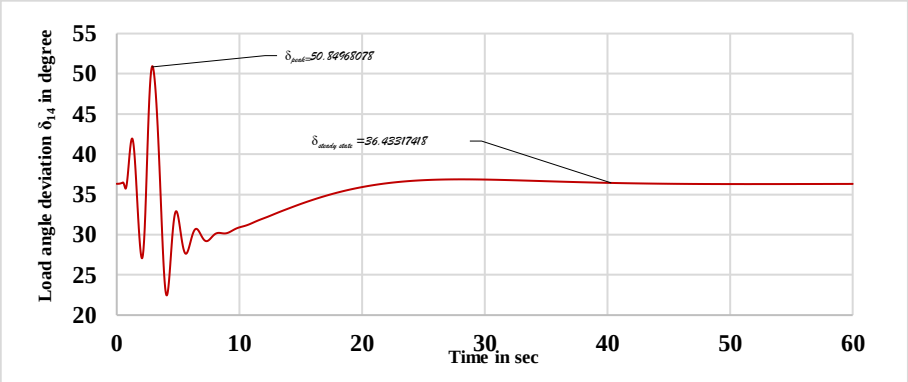

Figure 17. Power angle (δ_{14}) with PSS

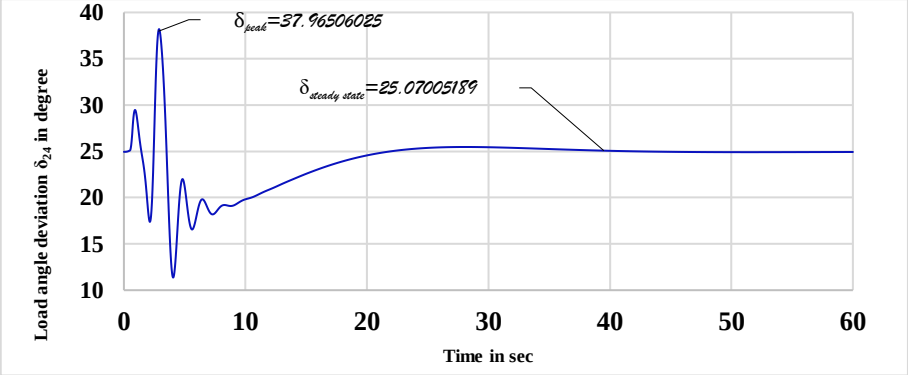

Figure 18. Power angle (δ_{24}) with PSS

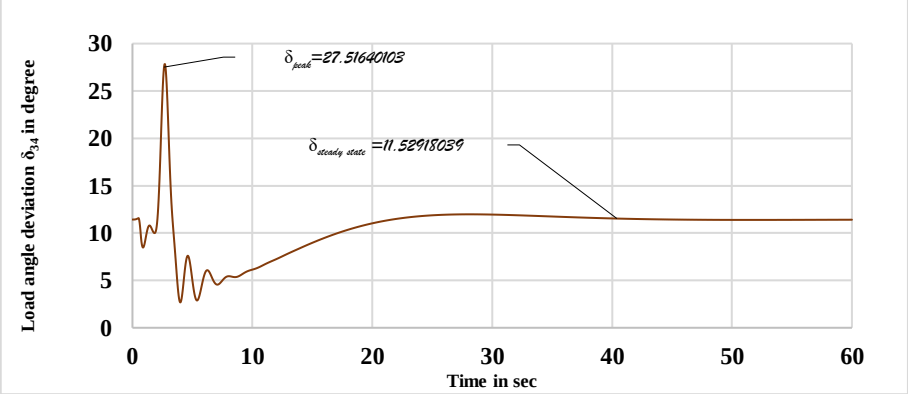

Figure 19. Power angle (δ_{34}) with PSS

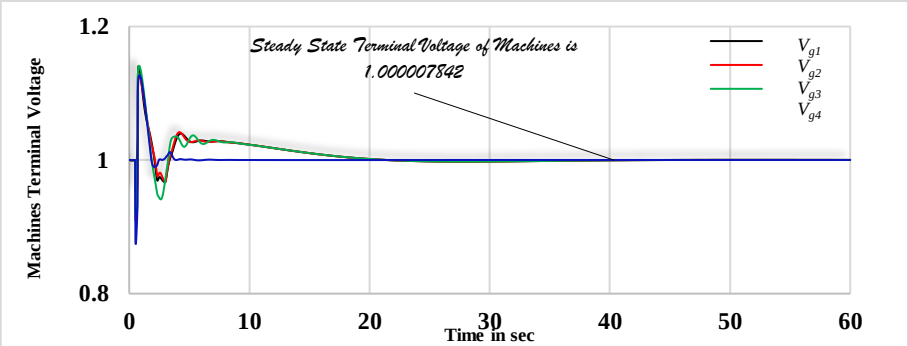

Figure 20. Terminal voltages of Machines without PSS

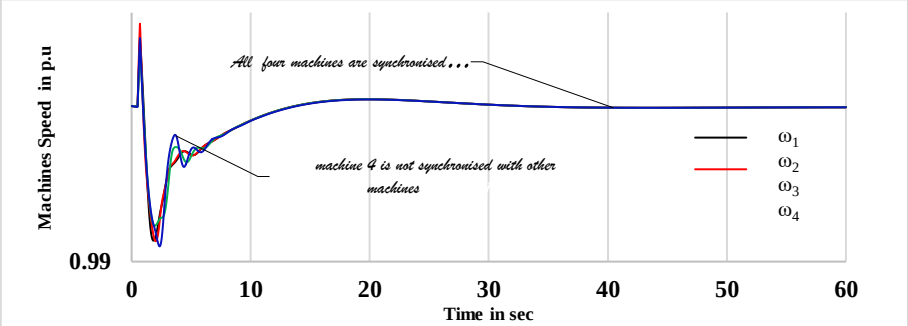

Figure 21. Machines Speed with PSS

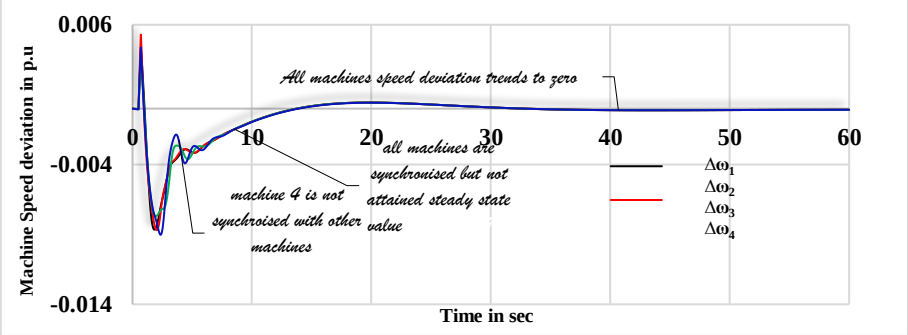

Figure 22. Machines Speed Deviation with PSS

7.1.3. Case 3

The fuzzy logic-based PSS is used in this instance to drive the excitation system. Machine speed serves as one of the fuzzy logic's inputs, and as machine speed changes, corresponding control signals are sent via PSS to the excitation system. Figure 23-25 depicts the system's load angle. As can be seen, the load angle reaches steady state at t=20 sec, which is much better than example 2. As a result, the system load angle's associated steady state error is decreased.

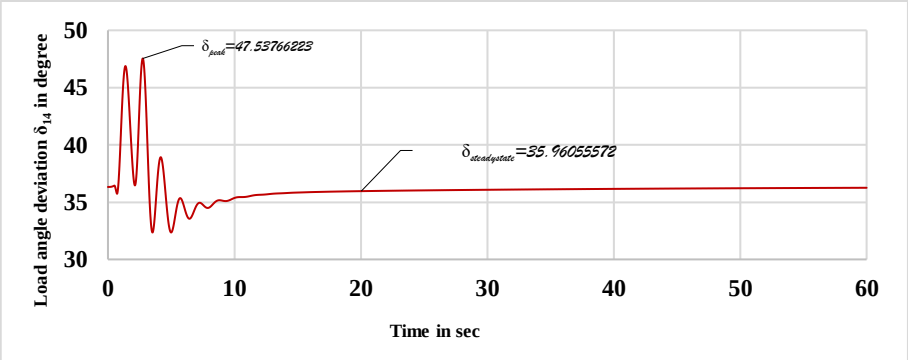

Figure 23. Power angle (δ_{14}) with PSS with Fuzzy based PSS

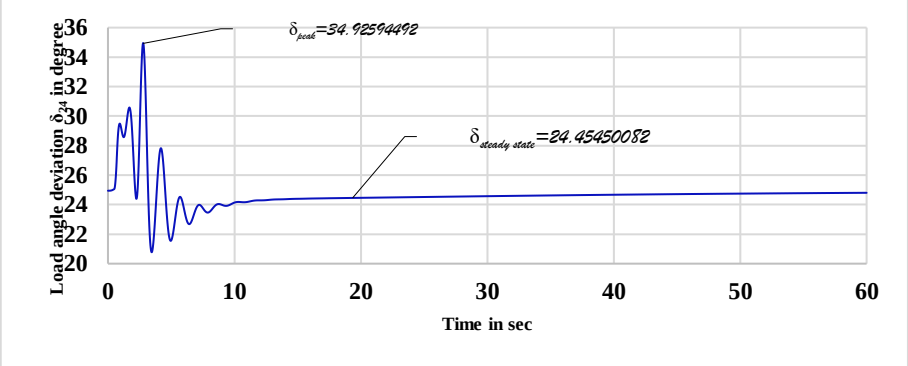

Figure 24. Power angle (δ_{24}) with PSS with Fuzzy based PSS

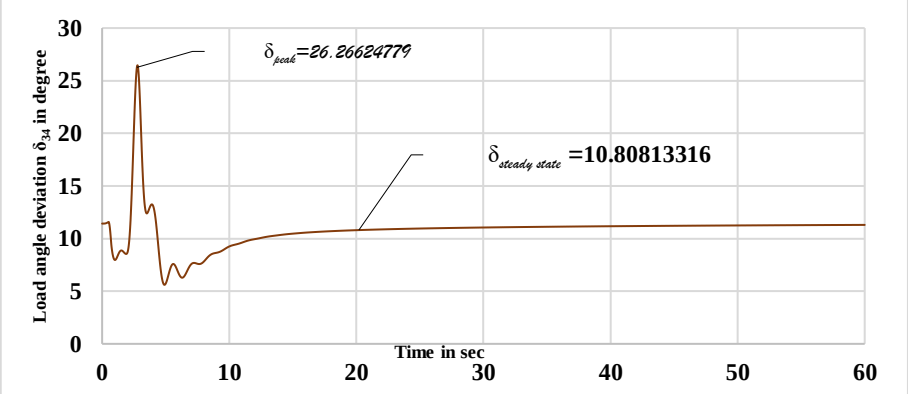

Figure 25. Power angle (δ_{24}) with PSS with Fuzzy based PSS

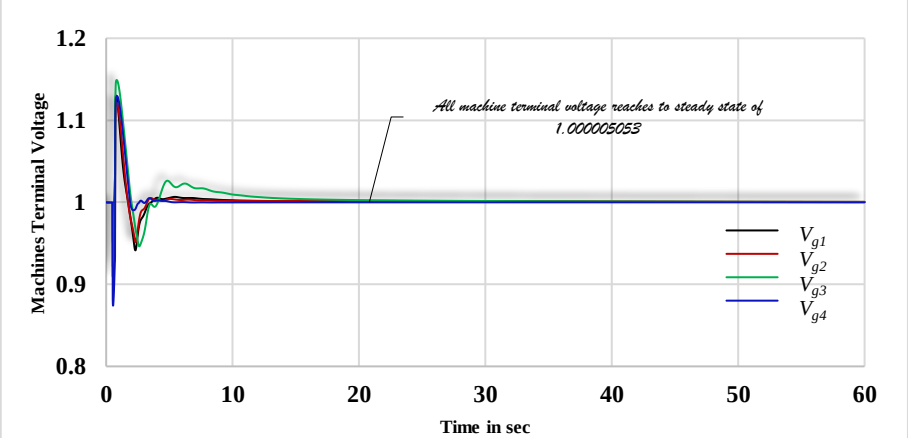

Figure 26. Terminal voltages of Machines with Fuzzy based PSS

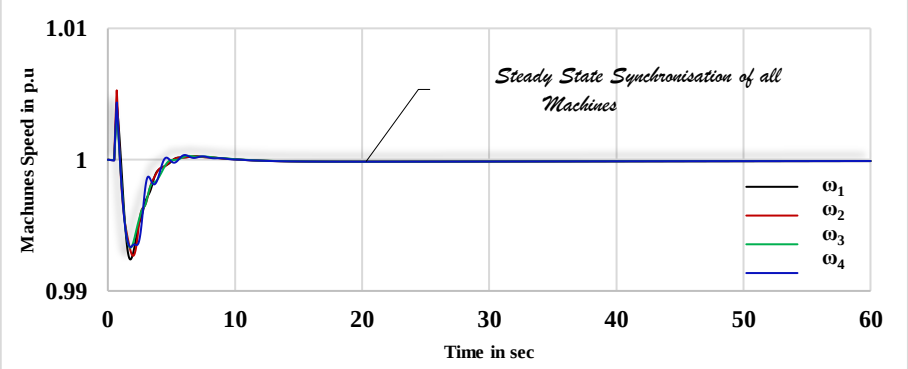

Figure 27. Machines Speed with Fuzzy based PSS

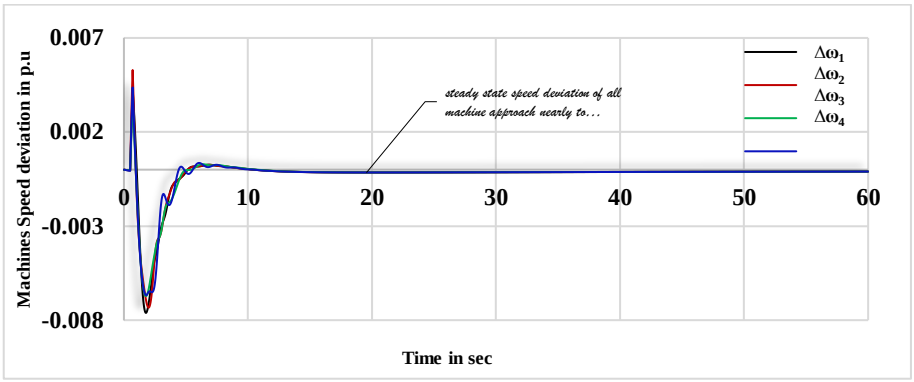

Figure 28. Machine Speed Deviation with Fuzzy based PSS

Compared to cases 1 and 2, the machines' terminal voltage oscillates and returns to its nominal value more quickly. In other words, at time t=20 sec, the terminal voltage of the devices reaches steady state. Figure 26 shows how the system's voltage response is better than in earlier instances.

Once the fault is created and the machines lose their synchronism, we can see that they are not synchronised. Following the dampening of the load angle variation, the associated machines retain synchronism until it reaches its steady state at t=20sec, as shown in Figure 27. Compared to case 2, the response to a machine speed variance is quicker. From the perspective of stability, the speed deviation of the machine while maintaining this parameter within acceptable bounds plays a significant role in satisfying the synchronism restrictions. In this instance, the machine's speed deviation should be zero, but in practise, it is measured in milli rad/sec. Yet reducing this variance is our major goal. Figure 28 shows that the machine speed divergence achieves zero at t=20 seconds.

7.1.4. Case 4: Fuzzy based PSS and STATCOM

In Figure 29 STATCOM is connected at bus 7, STATCOM is basically voltage source inverter connected in shunt fashion, STATCOM can inject constant current irrespective of terminal voltages to connected bus.

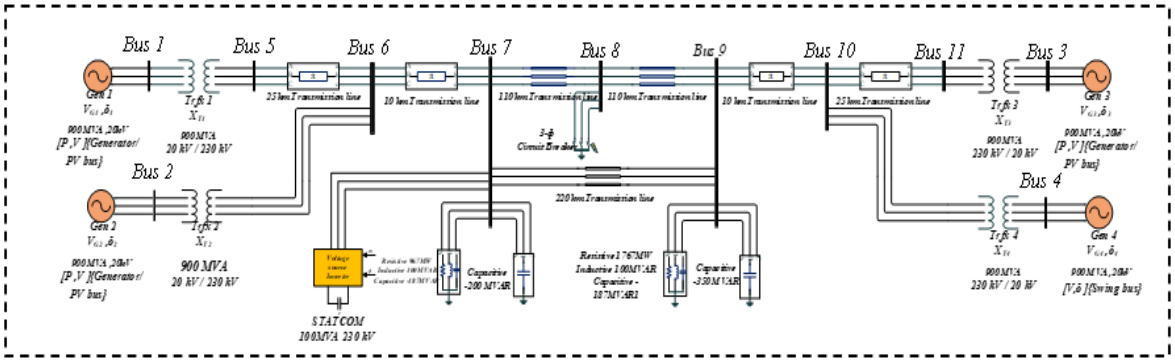

Figure 29. 4-Machine 11-Bus Test System with application of STATCOM

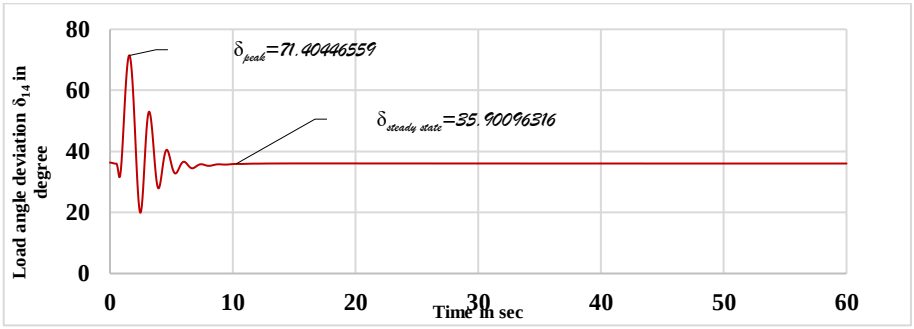

Figure 30. Power angle (δ_{14}) with PSS with Fuzzy based PSS and STATCOM

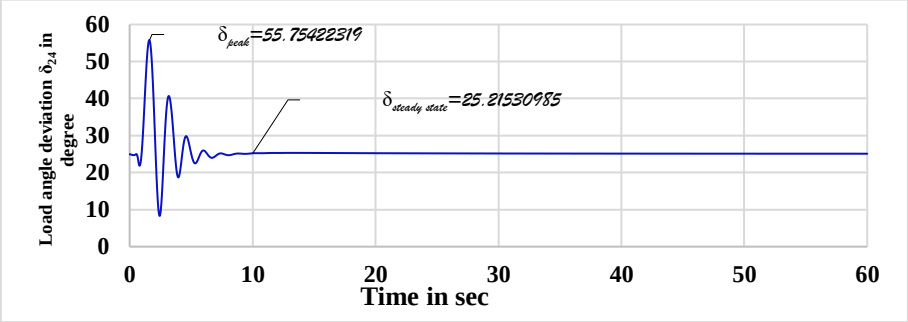

Figure 31. Power angle (δ_{24}) with PSS with Fuzzy based PSS and STATCOM

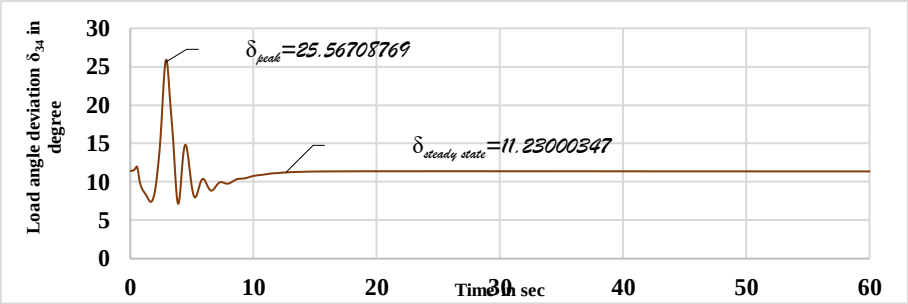

Figure 32. Power angle (δ_{34}) with PSS with Fuzzy based PSS and STATCOM

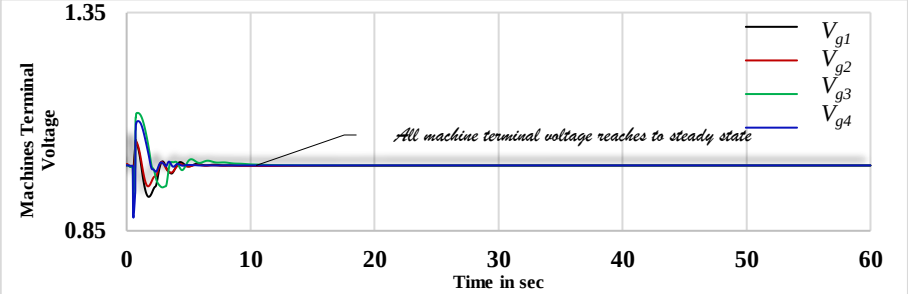

Figure 33. Terminal voltages of Machines with PSS and STATCOM

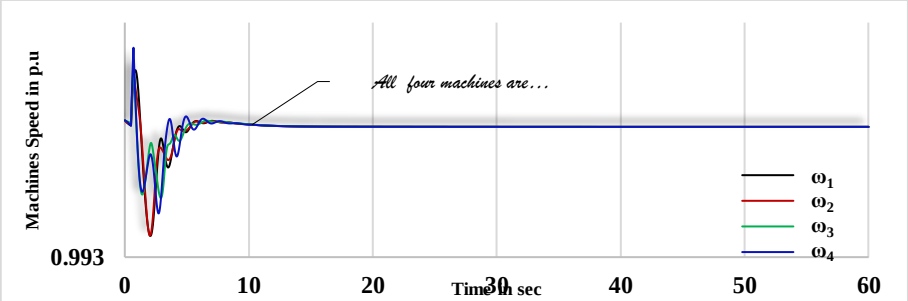

Figure 34. Machines Speed with Fuzzy based PSS with STATCOM

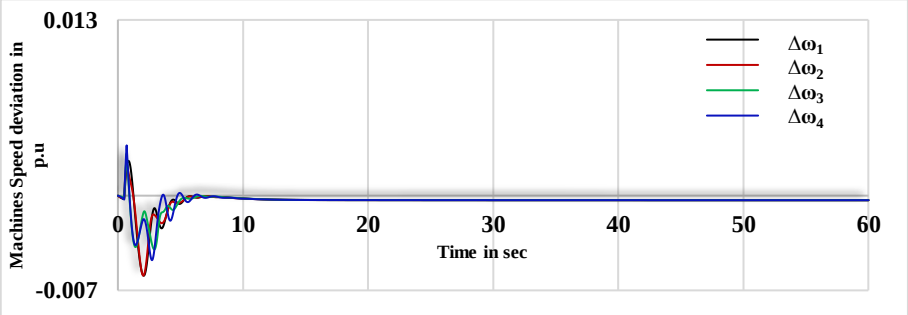

Figure 35. Machines Speed Deviation with Fuzzy based PSS with STATCOM

The primary advantage of FACTS devices is their capacity to increase the power system's damping, which can improve the network's stability. Figure 30-32 depicts the system load angle for case 4. It is plain to see that the effect of damping is greatly strengthened in this situation, and the system regains equilibrium at t=10 sec, which is much better than in cases 2 and 3. Figure 33 shows how the machine terminal voltage oscillates and levels off at time t=10. STATCOM and the fuzzy based PSS have both provided extra damping effects as indicated by Figures 34-35.

8. COMPARISON OF ALL FOUR CASE FOR STABILITY

Figure 36-38 shows the comparison of load angle deviations for all cases we considered in a single plot. From each figure shown base case is plot in dotted line (case 1), red solid (case 2), green solid line (case 3) and dark blue solid line (case 4). We can conclude by obtained results that case 4 is effective in damping of load angle deviation for the given power system network.

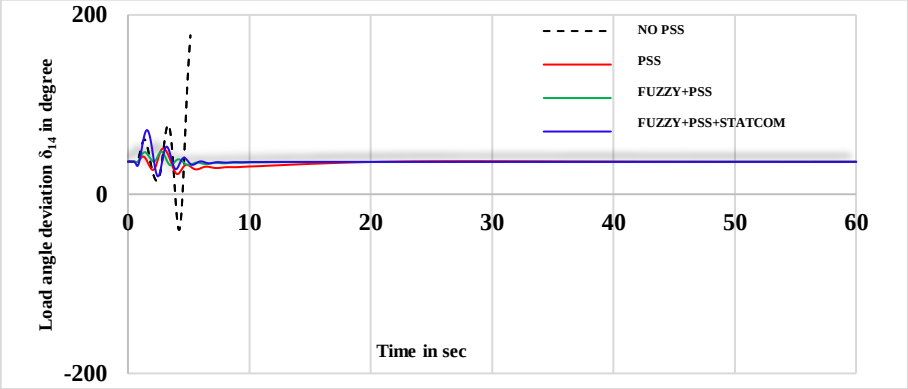

Figure 36. Comparison of Power angle (δ_{14}) for all four cases

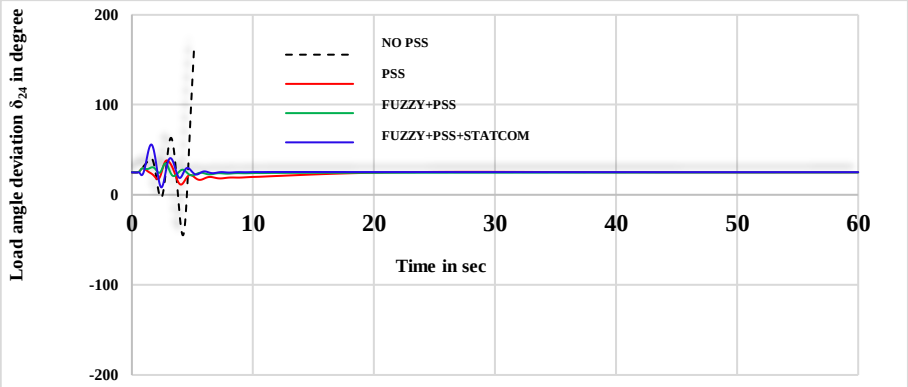

Figure 37. Comparison of Power angle (δ_{24}) for all four cases

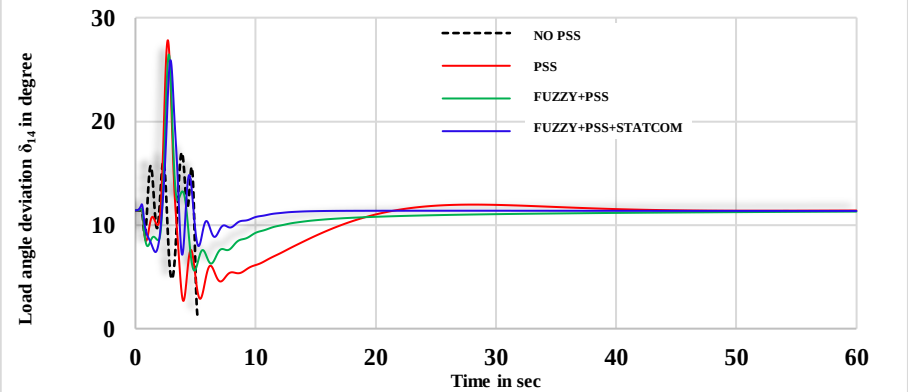

Figure 38. Comparison of Power angle (δ_{34}) for all four cases

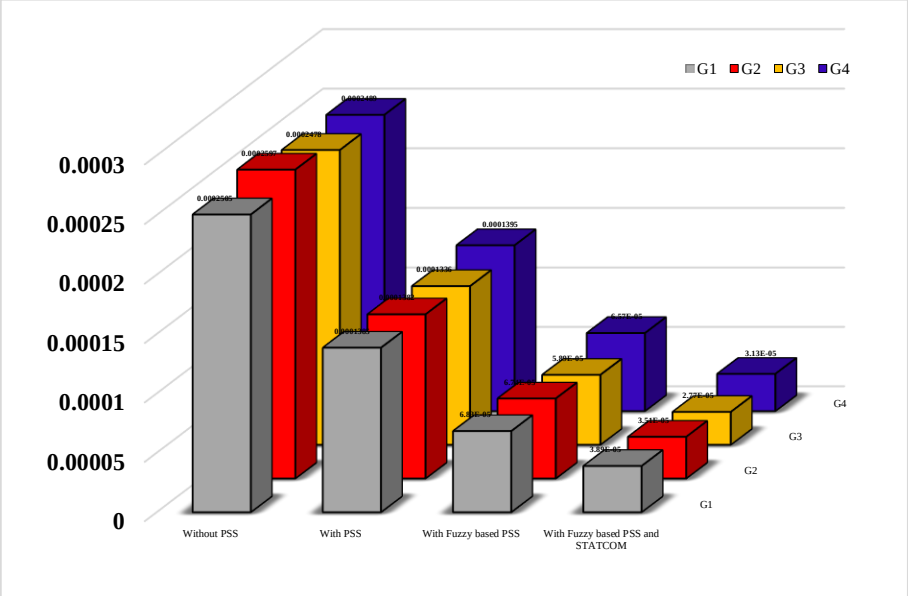

Figure 39. ISE of generator for all four cases for 3-ϕ 12-cycle fault

Table 3. Comparison of Integral Square Error of generator for all four cases

Generator	Integral Square Error(ISE) for 3-ϕ 12 cycle fault			
	Case-1	Case-2	Case-3	Case-4
G_1	0.0002505	0.0001385	6.828e-05	**3.894e-05**
G_2	0.0002597	0.0001382	6.737e-05	**3.510e-05**
G_3	0.0002478	0.0001336	5.889e-05	**2.766e-05**
G_4	0.0002489	0.0001395	6.569e-05	**3.131e-05**

Table 3 shows that the comparison of ISE of the generator speed deviation for case 1 we can observe that ISE error is more in the range of 0.0002489-0.0002597. In case 2 ISE in the range of 0.0001336-0.0001395. In case 3 ISE in the range of 5.889e-05 – 6.828e-05. However, in case 4 ISE is in the range of 2.766e-05 -3.894e-05. We can conclude that ISE is minimum in case 4. The physical meaning is that the machine speed deviation is minimum as compared to the other three cases. Figure 39 shows the graphical representation of the ISE of each generator for all 4 cases from the ISE is less in case 4 due to the presence of Fuzzy based PSS and STATCOM.

8.1. Proposed work is compared with compatible work

The proposed work is compared with the existing work in which they have done case study for 3-ϕ 5 cycle fault. We have done the extension for the same case and compared with the Fuzzy Rules Matrix [FRM] based research article. The performance indices which is ISE of proposed case-3 and proposed case-4 is compared with the FRM [29, 30].

Table 4. Compatible work and its application

Ref no.	Test system	Application	Controller	Stability
[29]	4-Machine 2 Area	Damped Low Frequency Oscillation	FRM [29]	Stable
[30]	4-Machine 2 Area	Damped Low Frequency Oscillation	FRM [30]	Stable
Proposed Case 3	4-Machine 2 Area	Damped Low Frequency Oscillation	Fuzzy PSS	Stable
Proposed Case 4	4-Machine 2 Area	Damped Low Frequency Oscillation	Fuzzy PSS	Stable

Table 5. Comparison with compatible work

Generator	Integral Square Error(ISE) for 3-ϕ 5 cycle fault			
	FRM[29]	FRM[30]	Proposed Case-3	Proposed Case-4
G_1	6.0986E-06	6.0180E-06	**3.062E-06**	**2.973E-06**
G_2	4.2193E-06	4.1759E-06	**3.464E-06**	**2.991E-06**
G_3	2.0780E-05	2.0690E-05	**2.509E-06**	**2.401E-06**
G_4	1.5150E-05	1.5112E-05	**2.839E-06**	**2.58E-06**

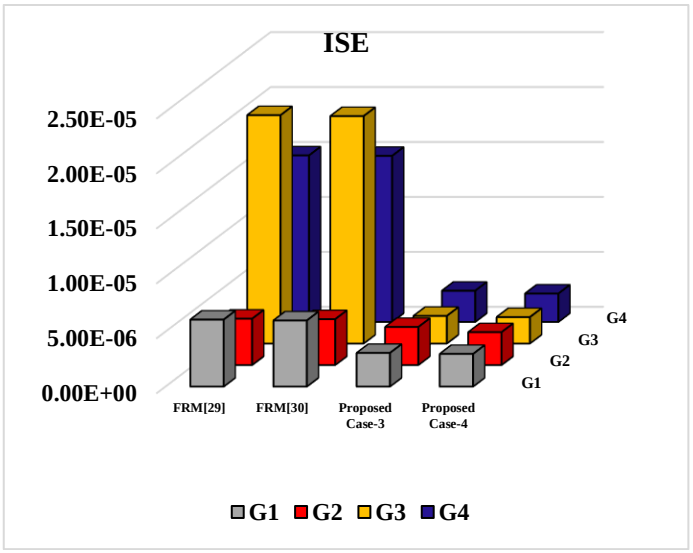

Figure 40. ISE of generator for all four cases for 3-ϕ 5-cycle fault

In Table 4 the Fuzzy rule matrix based PSS designed which is taken as the compatible work for the proposed work the application is of damping the low frequency oscillation in that case study they have considered standard IEEE 11 bus power system network. For the stability enhancement of multimachine system the performance indices play a vital role. In that Integral square error is taken into account for the comparing with the compatible work.

Table 5 shows that the performance indices i.e., ISE of FRM [29] & FRM [30] more which means that, there is a more speed deviation of generator in the considered IEEE 11 bus system, whereas the proposed fuzzy controller with case-3 & case-4 is less, due the less speed deviation of generator the stability of multimachine is enhanced, corresponding bar graph of ISE of of generator for all four cases as shown in Figure 40.

9. CONCLUSION

To damp out the rotor oscillation in the power system network and to minimize the Integral Square Error of machine speed deviation, coordination damping, i.e., Fuzzy based PSS and STATCOM is proposed. From this coordination damping power system stability enhancement is achieved by maintaining the generator terminal voltage within the limits and load angle deviation of the system is maintained constant after damping out of rotor oscillation, machines attain synchronism within less time once the 3-ϕ, 12 cycle fault has been cleared. Comparison with the compatible work have been done by creating 3-ϕ, 5 cycle fault the corresponding performance indices ISE is compared with the existing technique and hence conclude that the proposed work will enhance the stability of multimachine system as compared to existing technique.

FUTURE SCOPE

The same fuzzy based controller in PSS is tested on different IEEE test system for different FACTS devise like SSSC and UPFC.

TERMINOLOGY

R_s	Stator resistance in p. u	ω	Angular speed of generator in rad per second
X_q	q-axis reactance in p.u	ω_s	Generator synchronous speed in rad per second
X_q'	Transient q-axis reactance in p.u	T_{qo}'	q-axis time constant associated with E_d' in second
X_q''	Sub-Transient q-axis reactance in p.u	T_{qo}''	q-axis time constant associated with Ψ_{2d} in second
X_d	d-axis reactance in p.u	T_{do}'	d-axis time constant associated with E_q' in second
X_d'	Transient d-axis reactance in p.u	T_{do}''	d-axis time constant associated with Ψ_{1d} in second
X_d''	Sub-Transient d-axis reactance in p.u	T_A	Amplifier time constant in second
H	Shaft inertia constant in second	C	DC link capacitor.
E_q'	q-axis transient internal voltages in p.u	I_{dc}	Current through capacitor.
E_d'	d-axis transient internal voltages in p.u	I_{sd}	d-axis component of STATCOM current
Ψ_{1d}	Damper winding 1d flux linkages in p.u	I_{sq}	q-axis component of STATCOM current
Ψ_{2d}	Damper winding 2q flux linkages in p.u	A	State matrix
E_{fd}	Field voltage in p.u	X	State vector
R_F	Rate feedback in p.u	B	Input matrix
T_{Fw}	Frictional windage torques	U	Control vector
δ	Rotor angle or load angle in rad		

APPENDIX

GENERATOR DATA

Parameter Names	Generator-1	Generator-2	Generator-3	Generator-4
[X_d X_d' X_d'' X_q X_q' X_q'' X_l]	[1.8 .3 .25 1.7 .55 .25 .2]	[1.8 .3 .25 1.7 .55 .25 .2]	[1.8 .3 .25 1.7 .55 .25 .2]	[1.8 .3 .25 1.7 .55 .25 .2]
[P_n(VA) V_n(Vrms) f_n(Hz)]	[900E6 20000 60]	[900E6 20000 60]	[900E6 20000 60]	[900E6 20000 60]
[T_{do}' T_{do}'' T_{qo}' T_{qo}''] (s)	[8 .03 .4 .05]	[8 .03 .4 .05]	[8 .03 .4 .05]	[8 .03 .4 .05]
P (W)	700000000	-	719000000	700000000
Generator Type	PV	Swing	PV	PV
Rotor Type	Round	Round	Round	Round

STATCOM DATA

Power Rating	100	Controller mode	Voltage regulation
Nominal Voltage	2300	Droop	0.03
Frequency	60	Capacitor	325
Converter Resistance	0.00733	Ac voltage regulator gains [k_{acp} , k_{aci}]	[5, 1000]
Converter Inductance	0.22	Dc voltage regulator gains [k_{dcp} , k_{dci}]	[0.001, 0.02]
DC Link voltage	40	Current regulator gain [k_{crp} , k_{cri} , k_{crf}]	[0.3 ,10 ,0.22]

REFERENCES

[1] Kundur, P. (2006). Power System Stability and Control. New Delhi: Tata McGraw, https://www.mheducation.co.in/power-system-stability-andcontrol-9780070635159-india

[2] N. Hatziargyriou et al., "Definition and Classification of Power System Stability Revisited & Extended," in IEEE Transactions on Power Systems, doi: 10.1109/TPWRS.2020.3041774.

[3] A. Kanchanaharuthai, V. Chankong and K. A. Loparo, "Transient Stability and Voltage Regulation in Multimachine Power Systems Vis-à-Vis STATCOM and Battery Energy Storage," in IEEE Transactions on Power Systems, vol. 30, no. 5, pp. 2404-2416, Sept. 2015, doi: 10.1109/TPWRS.2014.2359659.

[4] Kumar, S., Kumar, A. & Sharma, N.K. Sensitivity analysis-based performance and economic operation of wind-integrated system with FACTS devices for optimum load dispatch. *Renewables* **4,** 2 (2017). https://doi.org/10.1186/s40807-017-0039-7

[5] Dash, P.K., Patnaik, R.K. & Mishra, S.P. Adaptive fractional integral terminal sliding mode power control of UPFC in DFIG wind farm penetrated multimachine power system. *Prot Control Mod Power Syst* **3,** 8 (2018). https://doi.org/10.1186/s41601-018-0079-z

[6] I. Kamwa, R. Grondin and G. Trudel, "IEEE PSS2B versus PSS4B: the limits of performance of modern power system stabilizers," in IEEE Transactions on Power Systems, vol. 20, no. 2, pp. 903-915, May 2005, doi: 10.1109/TPWRS.2005.846197.

[7] Mohsen Bakhshi, Mohammad Hosein Holakooie, Abbas Rabiee,Fuzzy based damping controller for TCSC using local measurements to enhance transient stability of power systems,International Journal of Electrical Power & Energy Systems,Volume 85,2017,Pages 12-21,ISSN 0142-0615,https://doi.org/10.1016/j.ijepes.2016.06.014.
[8] W. Yao, L. Jiang, J. Wen, Q. H. Wu and S. Cheng, "Wide-Area Damping Controller of FACTS Devices for Inter-Area Oscillations Considering Communication Time Delays," in IEEE Transactions on Power Systems, vol. 29, no. 1, pp. 318-329, Jan. 2014, doi: 10.1109/TPWRS.2013.2280216.
[9] Graham Rogers, ''Power System Structure and Oscillations" Springer, 2000, ISBN : 978-1-4613-7059-8
[10] H. Zamani, M. Karimi-Ghartemani, and M. Mojiri, ''Analysis of power system oscillations from PMU data using an EPLL-based approach,''*IEEE Trans. Instrum. Meas.*, vol. 67, no. 2, pp. 307–316, Feb. 2018
[11] Essallah, S., Bouallegue, A. & Khedher, A. Integration of automatic voltage regulator and power system stabilizer: small-signal stability in DFIG-based wind farms. *J. Mod. Power Syst. Clean Energy* **7,** 1115–1128 (2019). https://doi.org/10.1007/s40565-019-0539-0
[12] Hemeida, M.G., Rezk, H. & Hamada, M.M. A comprehensive comparison of STATCOM versus SVC-based fuzzy controller for stability improvement of wind farm connected to multi-machine power system. *Electr Eng* **100,** 935–951 (2018). https://doi.org/10.1007/s00202-017-0559-6
[13] Karpagam, N., Devaraj, D. & Subbaraj, P. Improved fuzzy logic controller for SVC in power system damping using global signals. *Electr Eng* **91,** 395–404 (2010). https://doi.org/10.1007/s00202-010-0148-4
[14] Peres, W. Multi-band power oscillation damping controller for power system supported by static VAR compensator. *Electr Eng* **101,** 943–967 (2019). https://doi.org/10.1007/s00202-019-00830-9
[15] Sundaramoorthy, K., Thomas, V., O'Donnell, T. *et al.* Virtual synchronous machine-controlled grid-connected power electronic converter as a ROCOF control device for power system applications. *Electr Eng* **101,** 983–993 (2019). https://doi.org/10.1007/s00202-019-00835-4
[16] Dey, P., Saha, A., Bhattacharya, A. *et al.* Analysis of the Effects of PSS and Renewable Integration to an Inter-Area Power Network to Improve Small Signal Stability. *J. Electr. Eng. Technol.* **15,** 2057–2077 (2020). https://doi.org/10.1007/s42835-020-00499-2
[17] Feng, S., Wu, X., Wang, Z. *et al.* Damping forced oscillations in power system via interline power flow controller with additional repetitive control. *Prot Control Mod Power Syst* **6,** 21 (2021). https://doi.org/10.1186/s41601-021-00199-7
[18] Du, W., Wang, H. & Cheng, S. A novel method to analyze damping effect of VSC based FACTS. *Sci. China Ser. E-Technol. Sci.* **51,** 2112–2119 (2008). https://doi.org/10.1007/s11431-008-0244-0
[19] Karpagam, N., Devaraj, D. & Subbaraj, P. Improved fuzzy logic controller for SVC in power system damping using global signals. *Electr Eng* **91,** 395–404 (2010). https://doi.org/10.1007/s00202-010-0148-4
[20] Ayyarao S. L. V. Tummala, Hemanth K. R. Alluri & P. V. Ramanarao (2020) Optimal Control of DFIG Wind Energy System in Multi-machine Power System using Advanced Differential Evolution, IETE Journal of Research, 66:1, 91-102, DOI: 10.1080/03772063.2018.1466732
[21] Hui Li, Shengquan Liu, Haiting Ji, Dong Yang, Chao Yan Hongwen Chen, Bin Zhao, Yaogang Hu, Zhe Chen,Damping control strategies of inter-area low-frequency oscillation for DFIG-based wind farm integrated into a power system,International Journal of Electrical Power & Energy Systems,Volume 61,2014,Pages 279-287,ISSN 0142-0615,https://doi.org/10.1016/j.ijepes.2014.03.009.
[22] X. He and H. Geng, "Transient Stability of Power Systems Integrated With Inverter-Based Generation," in *IEEE Transactions on Power Systems*, vol. 36, no. 1, pp. 553-556, Jan. 2021, doi: 10.1109/TPWRS.2020.3033468.
[23] H. N. V. Pico and B. B. Johnson, "Transient Stability Assessment of Multi-Machine Multi-Converter Power Systems," in IEEE Transactions on Power Systems, vol. 34, no. 5, pp. 3504-3514, Sept. 2019, doi: 10.1109/TPWRS.2019.2898182.
[24] E. Vittal, M. O'Malley and A. Keane, "Rotor Angle Stability With High Penetrations of Wind Generation," in IEEE Transactions on Power Systems, vol. 27, no. 1, pp. 353-362, Feb. 2012, doi: 10.1109/TPWRS.2011.2161097.
[25] L.O. Mak, Y.X. Ni, C.M. Shen,STATCOM with fuzzy controllers for interconnected power systems,Electric Power Systems Research,Volume 55, Issue 2,2000,Pages 87-95,ISSN 0378-7796, https://doi.org/10.1016/S0378-7796(99)00100-5.
[26] I. Abdulrahman and G. Radman, "Simulink-Based Program for Simulating Multi- Machine Power Systems," 2018 IEEE Power & Energy Society General Meeting (PESGM), Portland, OR, USA, 2018, pp. 1-5, doi: 10.1109/PESGM.2018.8585773.
[27] M. Aghazadeh Tabrizi and G. Radman, "PMU-based multi-input SVC supplementary controller for damping inter-area oscillation," North American Power Symposium 2010, Arlington, TX, USA, 2010, pp. 1-6, doi: 10.1109/NAPS.2010.5618948.
[28] M. J. Morshed and A. Fekih, "A Coordinated Controller Design for DFIG-Based Multi-Machine Power Systems," in IEEE Systems Journal, vol. 13, no. 3, pp. 3211-3222, Sept. 2019, doi: 10.1109/JSYST.2018.2872411.
[29] Miguel Ramirez-Gonzalez & O. P. Malik (2010) Self-tuned Power System Stabilizer Based on a Simple Fuzzy Logic Controller, Electric Power Components andSystems, 38:4, 407423, DOI: 10.1080/15325000903330591
[30] Dhanesh Kumar Sambariya & Rajendra Prasad (2017) A Novel Fuzzy Rule Matrix Design for Fuzzy Logic-based Power System Stabilizer, Electric Power Components and Systems, 45:1, 34-48, DOI: 10.1080/15325008.2016.1234008.
[31] P. W. Sauer and M. A. Pai, "Power System Dynamics and Stability," Prentice-Hall, Inc., New Jersey, USA, 1998.

BIOGRAPHY OF AUTHORS

Madhusudhan M was born in Mysore/India on 13th of January 1995. He received his B.E in Electrical & Electronics Engineering in 2017 from Vidya Vardhaka College of Engineering Mysore/India. He finished his M.Tech Degree in Power System Engineering in 2019 from The National Institute of Engineering Mysore/India. Currently he his 4th year pursing full time Ph.D under NDF AICTE scheme under Visvesvaraya Technological University. His main field of research optimization in power system. Power system Stability, FACTS controller and Power system stabilizer for Damping Power system oscillation
Email: madhusudhanm2015@gmail.com

Dr. Pradeepa H received PhD degree in Electrical & Electronics Engineering in 2019 from Visvesvaraya Technological University. He received his master degree from NITK Surathkal/India in the year 2005. Currently he is working as Head of the Department of Electrical & Electronics Engineering at The National Institute of Engineering. He has 14 journal and 7 conference papers under his guidance Two NDF Research scholar Pursuing full time Ph.D under Visvesvaraya Technological University. His area of research are Energy Management System, Power System Protection and Power System Optimization.
Email: pradeep3080@nie.ac.in

Dr. Likith Kumar M V his primary research interest is in the area of electrical power distribution system which includes distribution system state estimation, renewable integration and smart grid. During my PhD at The National Institute of Engineering, my research focus was on monitoring and control of distribution system integrated with distributed generation.
Email: likith@nie.ac.in

Srishail K Bilgundi, born in Karnataka, India, received Bachelor of Engineering degree from PDA college of Engineering in 2015 and Master of Technology degree from The National Institute of Engineering, Mysuru in 2017. Currently pursuing Ph.D. as full-time research scholar in the Department of Electrical and Electronics Engineering at The National Institute of Engineering, Mysuru, Karnataka, India under Visvesvaraya Technological University Belgaum. Area of research is Power Systems which includes distributed energy resources, renewable energy, power quality, FACTS, energy management and smart grid.
Email: sbilgundi7@gmail.com.